

miR-10a overexpression is associated with NPM1 mutations and MDM4 downregulation in intermediate-risk acute myeloid leukemia

Dmitriy Ovcharenko^{a,b,*}, Friedrich Stölzel^{c,*}, David Poitz^d, Fernando Fierro^c, Markus Schaich^c, Andreas Neubauer^e, Kevin Kelnar^a, Timothy Davison^a, Carsten Müller-Tidow^f, Christian Thiede^c, Martin Bornhäuser^c, Gerhard Ehninger^c, David Brown^a, and Thomas Illmer^c

^aAsuragen Inc., Austin, Tx., USA; ^bAltogen Labs, Austin, Tex., USA; ^cMedizinische Klinik und Poliklinik I, Dresden University of Technology, Dresden, Germany; ^dKlinik für Kardiologie, Dresden University of Technology, Dresden, Germany; ^eKlinik für Innere Medizin, Hämatologie, Onkologie, und Immunologie, University Hospital, Giessen and Marburg and Philipps University, Marburg, Germany; ^fKlinik für Innere Medizin, Hämatologie und Onkologie, University of Münster, Germany

(Received 2 February 2011; revised 5 June 2011; accepted 1 July 2011)

Parts of the study were presented at the Annual Meeting of the American Society of Hematology 2006 in Orlando, FL.

Objective. The study investigated differential microRNA (miRNA) expression patterns in acute myeloid leukemia (AML) patients with intermediate-risk (IR) characteristics. After characterization and validation of *miR-10a*, which was specifically upregulated in nucleophosmin 1 (*NPM1*) mutant AML samples, functional consequences of *miR-10a* overexpression were further delineated in vitro.

Materials and Methods. Microarray analysis of miRNAs in bone marrow samples from AML (IR) patients with *NPM1* mutations and healthy donors was performed to detect differential expression patterns. After validation of miRNA expression specific for *NPM1* mutation in AML patients by quantitative reverse transcription polymerase chain reaction, a functional target gene search was conducted using complementary DNA microarray data from samples transfected with *miR-10a*. Potential target gene validation was done using transient transfection of K562 cells followed by Western blotting and luciferase reporter assay.

Results. In comparison with wild-type samples, *NPM1* mutant AML samples were shown to markedly overexpress *miR-10a*. Subsequent in vitro *miR-10a* overexpression induced differential gene expression as determined by microarray analysis. Here the murine double minute 4 (*MDM4*) gene turned out as a candidate gene for *miR-10a*. Validation of *MDM4* in leukemic cells revealed a robust negative relationship between *miR-10a* overexpression and *MDM4* downregulation. Furthermore, we determined an inverse association between *miR-10a* and *MDM4* expression in AML (IR) samples with respect to their *NPM1* mutational status.

Conclusions. *miR-10a* expression is highly characteristic for AML (IR) patients with *NPM1* mutations and may influence its biological properties in AML by interfering with the *p53* machinery partly regulated by *MDM4*. © 2011 ISEH - Society for Hematology and Stem Cells. Published by Elsevier Inc.

Acute myeloid leukemia (AML) is a heterogeneous disease of hematopoietic stem cells and patients are often classified according to the presence of specific cytogenetic alterations [1].

*Drs. Ovcharenko and Stölzel contributed equally to this work.

Offprint requests to: Friedrich Stölzel, M.D., Medizinische Klinik und Poliklinik I, Universitätsklinikum Carl Gustav Carus der Technischen Universität, Fetscherstrasse 74, 01307 Dresden, Germany; E-mail: friedrich.stoelzel@uniklinikum-dresden.de

Supplementary data related to this article can be found online at doi: 10.1016/j.exphem.2011.07.008.

There are substantial differences in responses to treatments for various types of AML. Particular chromosomal aberrations that are frequently observed in AML blasts have been associated with treatment failure or relapse, such that the development of individualized treatment strategies tailored to patients presenting with specific genetic alterations is critical [2]. Historically, patients with normal karyotype have been defined as having intermediate-risk (IR) AML, although the course of disease progression in these individuals is highly variable [3]. Because of recent progress in the identification of genetic alterations associated with AML, the IR

designation is now further classified according to the presence of mutations in specific genes, such as those encoding Fms-like tyrosine kinase 3 (*FLT3*) [4], CCAAT/enhancer binding protein- α (*CEBP*/ α) [5], or nucleophosmin 1 (*NPM1*) [6]. Consequently, it is known that internal tandem duplications (ITD) of *FLT3* are associated with a poor prognosis [7–9], whereas *NPM1* mutations predict a positive response to chemotherapy [10–12]. Altered *FLT3* signaling is both specific and vital for the growth and survival of leukemic cells because inhibition of *FLT3* induces apoptosis in *FLT3*-ITD-positive cell lines [11,13,14]. Although direct inhibition of *NPM1* signaling has not been achieved, a number of studies have demonstrated the ability of mutated *NPM1* to counteract apoptosis, enhance self-renewal, and inhibit the differentiation of leukemic cells [15,16]. Moreover, *NPM1* mutations are associated with specific changes in the overall gene expression profile of myeloid cells [17,18], similar to that observed for *FLT3*-ITD mutations [19,20].

MicroRNAs (miRNAs) are small noncoding RNAs with cell-type-specific expression patterns [21]. They regulate expression of at least 5000 genes and represent one-third of the human genome [22]. miRNAs bind to partially or completely homologous sequences within the 3' untranslated region (3' UTR) of their mRNA targets and repress their expression at the post-transcriptional level (for review see [23]).

miRNAs are key players in genetic programs that control differentiation and embryogenesis, primarily by regulating expression of gene clusters that ultimately modulate cellular functions [24,25]. For example, overexpression of certain miRNAs is capable of driving the development of stem cells into lymphocytic and myeloid differentiation [26–28]. Similarly, changes in miRNA expression in response to the differentiating agent retinoic acid provides further evidence for the ability of miRNAs to regulate differentiation and proliferation of hematopoietic cells [29]. Interestingly, AML and acute lymphoblastic leukemia (ALL) patients can be discriminated by the expression profiles of miRNAs, which could prove to be more sensitive than screening with complementary DNA microarrays [29–31].

It is currently accepted that chromosomal abnormalities critically influence miRNA expression levels. For example, chromosomal translocation deregulates *miR-142* expression in t(8;17)-positive prolymphocytic leukemia [32] and *miR-223* expression in t(8;21)-positive AML [33]. Furthermore, *miR-10a* overexpression in *NPM1* mutant AML samples has recently been described [34]. Because the majority of AML patients do not have karyotypic alterations, we investigated AML patients with IR characteristics for specific alterations in miRNA expression in order to delineate the molecular consequences of these alterations.

Materials and methods

Patient characteristics and cell isolation

Bone marrow (BM) blast samples of AML patients with IR characteristics, included in the prospective AML96 and AML2003 trials of the Study Alliance Leukemia, were obtained at diagnosis by routine BM aspiration. The studies were approved by the institutional review board of the Medical Faculty of the Technical University, Dresden, Germany.

Mononuclear cells were isolated by density gradient centrifugation using Ficoll-Hypaque (1.077 g/mL) and cryopreserved in aliquots containing 5 to 20 $\times 10^6$ cells/sample. Normal BM samples were acquired from healthy donors, and mononuclear cells were prepared and cryopreserved. All donors gave written informed consent for the use of their samples, and all patients were homogeneously treated as described previously. Unmodified BM samples were further used for miRNA isolation as described for the microarray experiments. For quantitative reverse transcription polymerase chain reaction (qRT-PCR) experiments BM samples of healthy control donors were further processed. Isolation of CD34⁺ cells, CD3⁺ T cells and granulocytes was done as described previously [35].

AML risk classification

Chromosome analyses were performed as described previously [36]. The AML (IR) samples were classified as per the AML96 study, and samples from high- and low-risk patients were excluded. High-risk patients had $-5/\text{del}(5q)$, $-7/\text{del}(7q)$, hypodiploid karyotypes (except 45, X, $-Y$, or $-X$), inv(3q), abn112p, abn111q, +11, +13, +21, +22, t(6;9); t(9;22); t(9;11); t(3;3), or multiple aberrations. Low-risk patients had t(8;21).

Cell lines

Human AML cell lines HL-60, Kasumi-1, KG-1a, ME-1, MOLM-13, MV4-11, NB-4, OCI/AML3, THP-1, U-937, ALL-derived Jurkat, chronic myeloid leukemia in blast crisis-derived K-562, and cervix carcinoma HeLa (ATCC, LGC Standards, Wesel, Germany) were cultured in RPMI 1640 containing 10% fetal calf serum (FCS), except for OCI/AML3 cells, which were cultured in minimum essential medium- α containing 20% FCS. Exon 12 *NPM1* gene mutational status was described for all cell lines, except for K562 [37]. In K562, the exon 12 *NPM1* wild-type was found as described previously [12]. All-trans retinoic acid (ATRA; Sigma Aldrich, Munich, Germany) and tumor necrosis factor-related apoptosis-inducing ligand (TRAIL; Alexion, Cheshire, CT, USA) were used in concentrations of 2 μM and 100 ng/mL.

miRNA extraction

Total RNA isolation and small RNA enrichment were performed using the miRvana miRNA isolation kit (Ambion, Austin, TX, USA) according to manufacturer's instructions.

miRNA labeling and microarray analyses

Labeling and microarray hybridization were performed as described previously [38]. Briefly, purified miRNAs were labeled using the miRvana miRNA labeling kit (Ambion) and amine-reactive dyes, as recommended by the manufacturer. Poly(A) polymerase and a mixture of unmodified and amine-modified nucleotides were used to append a polynucleotide tail to the 3' end of each miRNA. The amine-modified miRNAs were coupled to NHS ester-modified Cy5 or Cy3 dyes (Amersham Bioscience, Piscataway, NJ, USA).

Unincorporated dyes were removed by a second glass-fiber filter-based cleaning procedure. Samples were independently labeled with Cy5 or Cy3 dyes, respectively. Absolute signal intensities for each spot were converted to relative intensities and converted to logarithm base 2 as $\text{Log}_2(\text{Cy5/Cy3})$. Each array was then centered by correcting the mean $\text{Log}_2(\text{Cy5/Cy3})$ ratio to zero to ensure all means of distributions of $\text{Log}_2(\text{Cy5/Cy3})$ within arrays is zero. This process was performed for each array.

Samples were hybridized for 12 to 16 hours at 42°C on prespotted glass slides. Thymus miRNA served as a hybridization control. For analysis of miRNAs in clinical samples, a microarray platform detecting 203 miRNA species was used (for detailed information see [Supplementary Table E1](#); online only, available at www.exphem.org). Following hybridization, the slides were scanned using a GenePix 4000B array scanner (MDC, Palo Alto, CA, USA), and each element was located and analyzed using the GenePix Pro 5.0 software package (Molecular Devices, Sunnyvale, CA, USA).

qRT-PCR

qRT-PCR was performed according to manufacturer’s instructions (Ambion) using approximately 20 pg miRNA per assay. Primer pairs included those for *miR-10a* and the murine double minute 4 (*MDM4*) gene (all primers were from Ambion). For the *MDM4* gene, we used assay Hs00159092_m1, amplifying parts of the exon 3 and 4 of the major splice variant of the *MDM4* gene (NM_2393.3, ENST00000367182).

Because there is no generally accepted normalization control for miRNA quantification, we investigated the impact of four different miRNAs as potential normalization controls (*5S*, *miR-24*, *miR-93*, and *miR-103*). Best correlations with the data observed in microarray experiments were determined using datasets normalized to *5S* RNA ([Supplementary Table E2](#); online only, available at www.exphem.org). We chose *5S* as the normalization control for miRNA for further quantification. mRNA expression was normalized to glyceraldehyde 3-phosphate dehydrogenase expression in the individual samples. The linearity of the assays was measured by dilution curve analysis, and the specificity of the assays was evaluated by melting curve analysis. Relative gene expression was calculated using the $2^{-\Delta\Delta\text{CT}}$ method [39].

Mutation detection

Mutations in the juxtamembrane domain of *FLT3* and exon 12 of *NPM1* were detected as described previously [9,12]. Patient samples were grouped according to the ratio of mutant (mut) to wild-type

(wt) *FLT3*-ITD in three groups as described previously (no mutation; $\text{mut/wt } FLT3\text{-ITD} \leq 0.8$; $\text{mut/wt } FLT3\text{-ITD} > 0.8$) [9].

Transfection of leukemic cells

Cells were washed with phosphate-buffered saline and suspended in hypo-osmolar electroporation buffer (Eppendorf, Hamburg, Germany) at 1.5×10^7 cells/mL, then *pre-miR-10a*, pre-miR precursor molecule-negative control, *anti-miR-10a*, anti-miR precursor molecule-negative control, or siAURKB (all 50 nmol), or siGAPDH (100 pmol) (all Ambion) were added to 100 μL aliquots OCI/AML3 or K562 cells. Cells were electroporated with one pulse at 240 V for 100 μs . These cells remained in the electroporation cuvettes for 5 to 10 minutes prior to culture for 24 and 48 hours in RPMI 1640, containing 10% FCS or minimum essential medium- α containing 20% FCS. A small RNA-expressing GFP (a generous gift of Dr. Brenner, Department of Pediatrics, Dresden University of Technology, Dresden, Germany) was used to determine transfection efficiency in OCI/AML3 and K562 cells prior to studies using *miR-10a* antisense or overexpression strategies. Transfection efficiency was determined by propidium iodide-based fluorescence-activated cell sorting analysis with transfection efficiencies of 50% to 60% in K562 cells and 20% for OCI/AML3 cells.

MTT assay

The MTT (3-(3,5-dimethylthiazol-2-yl)-2,5-diphenyl-tetrazoliumbromide) proliferation assay was performed as described previously [40].

DNA oligonucleotide microarray

DNA oligonucleotide microarrays (Affymetrix, Carlsbad, CA, USA) were performed as described previously [40].

Cloning of the miR-10a binding site from 3' UTR of MDM4

The putative *miR-10a* binding site within the 3' UTR of *MDM4* was identified using the Targetscan algorithm (targetscan.org) based on the NCBI transcript NM_002393.2. The wt or mutated binding sites, respectively, were cloned into the pMIRReporter vector (Ambion) via the *SpeI* and *HindIII* sites using the oligonucleotides (Eurofins MWG Operon, Ebersberg, Germany) described in [Table 1](#). Mutations of the binding site were performed by inverting the binding site (mutant 1) or by mutation of the seed sequence (mutant 2). The identity of all clones was verified by sequence analysis (Sequencing facility, MPI-CBG Dresden, Germany). The sequences of the used oligonucleotides are shown in [Table 1](#).

Table 1. Sequences of used oligonucleotides

| | | |
|---------------------|---|---|
| Wild-type sense | <i>SpeI</i> 5' - CTAGTGCTCAGCGGGAGGTGTGGGGCG ACAGGGTCA -3' | <i>HindIII</i> |
| Wild-type antisense | 3' - <u>ACGAGTCGCCCTCCACACCCCGCTGTCCCA</u> -5' | 5' - AGCTTGACCCTGTCGCCCCACACCTCCCGCTGAGCA -3' |
| Mutant 1 sense | <i>SpeI</i> 5' - CTAGTGCTCAGCCCCTCCACACCCCGCTG TCC CAG A -3' | <i>HindIII</i> |
| Mutant 1 antisense | 3' - <u>ACGAGTCGGGGAGGTGTGGGGCGACAGGGTCTTCGA</u> -5' | 5' - AGCTTCTGGGACAGCGGGGTGTGGAGGGGCTGAGCA -3' |
| Mutant 2 sense | <i>SpeI</i> 5' - CTAGTGCTCAGCGGGAGGTGTGGGGCG AAAAAACA -3' | <i>HindIII</i> |
| Mutant 2 antisense | 3' - <u>ACGAGTCGCCCTCCACACCCCGCTTTTTTTTGTTCA</u> -5' | 5' - AGCTTGTTTTTTTCGCCCCACACCTCCCGCTGAGCA -3' |

miR-10a seed match sequence in bold, mutated sequences are highlighted in grey background, and underlined type indicates the *SpeI* and *HindIII* restriction sites.

Transfection of MDM4 recombinants and luciferase assay

HeLa cells (2×10^5 cells/well) were seeded in 24-well plates (0.5 mL/well), and cotransfection of *MDM4* constructs (3'UTR/_wt/_mt1/_mt2) (0.4 μ g/mL), pre-miR-control-, anti-miR-control-, pre-miR-10a-, anti-miR-10a-miRNA (50 nmol), and Renilla (pRL-TK plasmid; Promega, Mannheim, Germany) (80 ng/mL) was performed in triplicates using Lipofectamine 2000-based transfection (Invitrogen, Carlsbad, CA, USA). At 48 hours after transfection, cells were lysed with passive lysis buffer (Promega) and the supernatant was collected. The Dual-Luciferase Reporter Assay System (Promega) was used according to manufacturer's instructions. Luminescence was measured using the Mithras LB 940 multimode reader (Berthold Technologies, Bad Wildbad, Germany). Pre-miR-control values were normalized; pre- and anti-miR-10a values were calculated in relation to the normalized pre-miR-control values and expressed as a relative percentage value.

Western blots

Proteins were isolated as described previously [41], and electrophoresis was performed by loading 30 μ g protein onto 12% acrylamide gels. Nitrocellulose membranes (BD Biosciences, San Jose, CA, USA) were incubated with primary antibodies specific for MDM4, glyceraldehyde 3-phosphate dehydrogenase, and actin (Santa Cruz Biotechnology, Santa Cruz, CA, USA; diluted 1:500) overnight at 4°C. Blots were washed and incubated with horseradish peroxidase-goat anti-mouse or anti-rabbit secondary antibodies (Dako, Glostrup, Denmark; diluted 1:2000). Western blots were developed by chemiluminescence using the ECL Plus Chemiluminescence Detection Kit (GE Healthcare, Uppsala, Sweden).

Statistical analysis

miRNA data were filtered for quality and significance using the Longhorn Array Database [42]. Filters were based on minimum intensity and pixel consistency. All data used for analysis had a signal-to-noise ratio >5 , an average sum intensity of 50% higher than that of the negative control spots, and a regression ratio >0.5 . Data were normalized globally per array such that the average LogRatio was 0 after normalization.

Hierarchical clustering of expression of 203 miRNAs was performed with average linkage and Pearson correlation. For the determination of differentially expressed miRNAs in leukemic (L) and normal-like (NL) samples, a two-sample *t*-test assuming equal variance was performed for every miRNA, and multiplicity correction [43] was performed to control the false discovery rate at 0.05%. Analysis of variance tests for the determination of differentially expressed miRNAs were performed using the Web-based GEPAS system [44].

Clinical variables of statistical significance were compared using the χ^2 -test for dichotomized variables and the Mann-Whitney *U*-test or Kruskal-Wallis H-test for continuous variables. Nonparametric correlations were performed to determine the correlation coefficient according to the Spearman rho test. Logistic regression analysis using multiple parameters was performed to identify the impact of single variables on the complete remission rate. Cox regression analysis was used to identify independent parameters associated with overall survival and relapse-free survival. The *p* values are two-sided, and a significance level of 0.05 was used. Clinical analyses were performed using SPSS version 16.0.1 (SPSS Inc, Chicago, IL, USA).

Results*Microarray analysis of miRNAs from AML (IR) patients*

We compared relative expression of 203 miRNAs in 21 AML samples with (IR) cytogenetics (for patients characteristics see [Supplementary Table E3](#); online only, available at www.expchem.org) with that of miRNAs in normal BM samples from five normal stem cell donors. Hierarchical cluster analysis demonstrated that most AML (IR) samples exhibited expression patterns different from those exhibited by normal BM samples ([Fig. 1A](#)). However, 5 of the 21 AML (IR) samples were not statistically different from normal BM samples. These samples were denoted as AML with NL miRNA expression and were subsequently compared with the L samples. Four of the five NL samples showed that the patients had *NPM1* mutation, despite the fact that they did not carry *FLT3*-ITD ([Supplementary Table E3](#); online only, available at www.expchem.org). Fourteen miRNAs were then identified with differential expression levels between NL and L samples ([Fig. 1B](#)). Most of these miRNAs were downregulated in the L samples compared with the NL samples. A number of miRNAs resembled candidates with previously annotated functional impact, such as *miR-10a*, *miR-16*, *miR-221*, *miR-223* and members of the oncomiR cluster on chromosome 13, including *miR-17-5p* and *miR-20* ([Table 2](#)). Results were validated comparing AML samples with normal hematopoietic cells by qRT-PCR. Here, the extraordinary high expression of *miR-10a* in AML samples could be verified, which is even higher, as in normal CD34⁺ cells. In contrast, expression differences for *miR-223* were more discrete and were therefore not studied further (see [Supplementary Figure E1](#); online only, available at www.expchem.org).

miR-10a overexpression in AML (IR) patients with NPM1 mutations

We therefore validated the findings for *miR-10a* in a larger subset of 89 AML (IR) samples. We detected no correlation between *miR-10a* expression for various clinical and laboratory parameters, albeit *miR-10a* expression strongly correlated with the presence of *NPM1* mutations in all patients ([Table 3](#)), although the highest expression levels were observed in patients who lacked *FLT3*-ITD mutation, despite being positive for *NPM1* mutation ([Fig. 2](#)). As expected, high *miR-10a* expression had a strong negative correlation with expression of the CD34 antigen on blast samples. We conclude that there is an unusually strong *miR-10a* overexpression in *NPM1* mutant AML samples.

Functional significance of elevated miR-10a expression

We characterized a subset of leukemic and nonleukemic cells with respect to *miR-10a* and *MDM4* expression. Investigation of cell lines for *miR-10a* demonstrated a marked *miR-10a* overexpression in OCI/AML3 cells with mutated

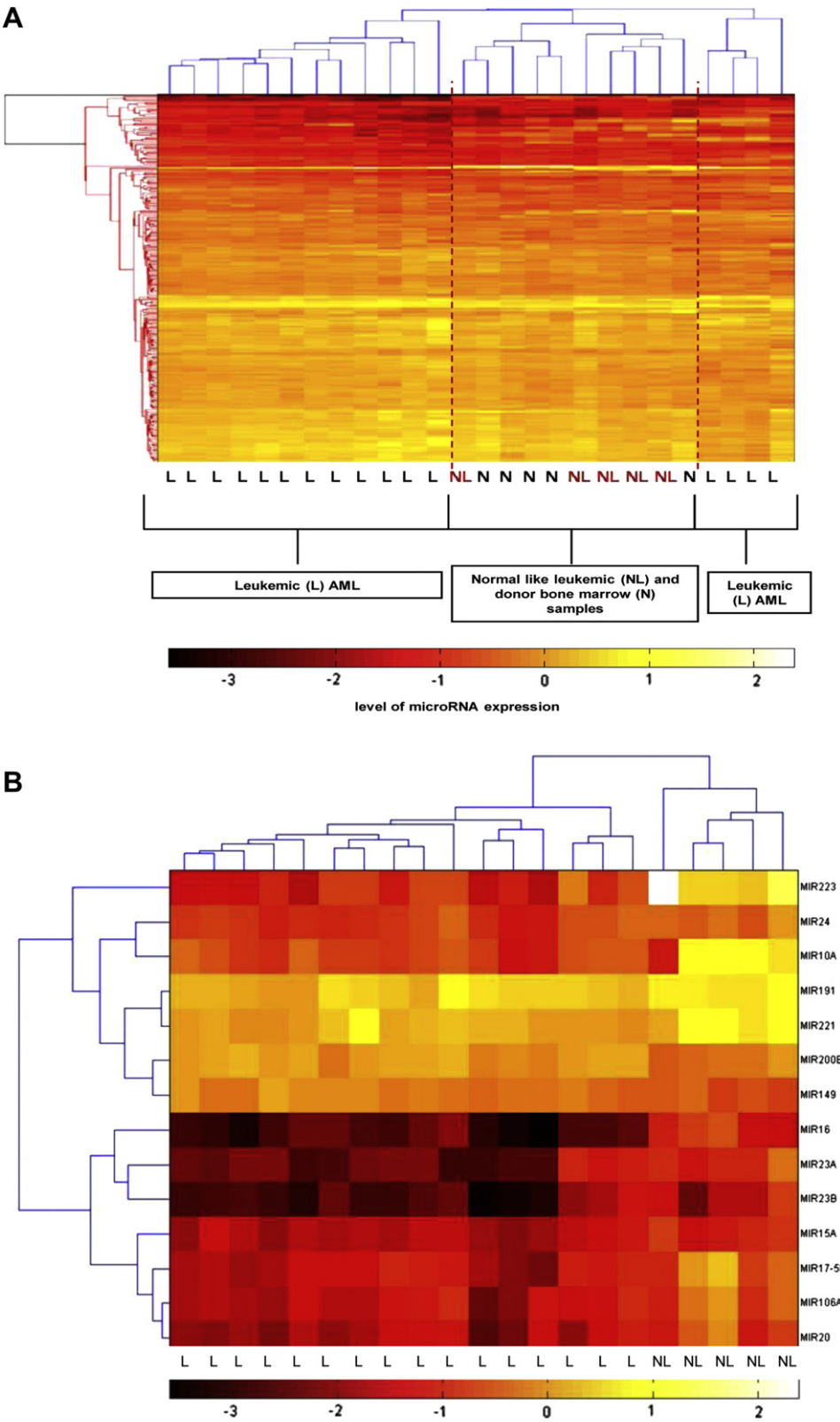


Figure 1. Differential miRNA expression in AML samples with (IR) cytogenetics. Hierarchical clustering of miRNA expression in AML samples with (IR) cytogenetics (L + NL) compared with that in normal bone marrow samples (N), samples in columns, miRNAs in rows. AML samples were denoted as either AML samples with aberrant miRNA profile (L = leukemic) or AML samples with a normal-like miRNA profile (NL = normal-like). (A) Heat map of AML (IR) miRNA expression profiles for 14 differentially regulated miRNAs comparing L and NL conditions, differential expression was determined for miRNA expression using *t*-test statistics and false discovery rate corrections (see Material and Methods).

Table 2. Comparison between differentially expressed miRNAs in AML (L) and (NL) samples

| miRNA | Expression in AML (L) samples | Chromosomal location | Function | Reference |
|------------------|-------------------------------|----------------------|---|-----------|
| <i>miR-223</i> | Down | Xq12 | Differentiation in granulopoiesis | [27] |
| <i>miR-24</i> | Down | | Inhibition of erythropoiesis, targeting of DHFR | [60,61] |
| <i>miR-24-1</i> | | 9q22.32 | | |
| <i>miR-24-2</i> | | 19p13.13 | | |
| <i>mir-10a</i> | Down | 17q21.32 | Tumor cell metastasis for <i>miR-10b</i> in breast cancer | [49] |
| <i>mir-191</i> | Down | 3p21.31 | Negative prognostic impact on AML patients | [29] |
| <i>mir-221</i> | Down | Xp11.3 | Downregulation of KIT and p27 (KIP1) in hematopoiesis and erythroleukemia | [62,63] |
| <i>mir-200B</i> | Up | 1p36.33 | Regulation of E-cadherin | [64] |
| <i>mir-149</i> | Up | 2q37.3 | Upregulation of KCNAB1 and LOX in clear cell renal cell carcinoma | [65] |
| <i>mir-16</i> | Down | | Regulation of BCL-2 in leukemia | [66] |
| <i>miR-16-1</i> | | 13q14.2 | | |
| <i>miR-16-2</i> | | 3q25.33 | | |
| <i>mir-23a</i> | Down | 19p13.12 | Hypoxia induced | [67] |
| <i>mir-23b</i> | Down | 9q22.32 | Regulation of HES1-mediated retinoic acid differentiation | [68] |
| <i>mir-15a</i> | Down | 13q14.2 | Regulation of BCL-2 in leukemia | [66] |
| <i>mir-17-5p</i> | Down | 13q31.3 | Part of an “oncomir” cluster, c-Myc-dependent E2F1 regulation | [69,70] |
| <i>mir-106a</i> | Down | Xq26.2 | Downregulation of RB1 in carcinogenesis | [71] |
| <i>mir-20a</i> | Down | 13q31.3 | Part of an “oncomir” cluster, c-Myc-dependent E2F1 regulation | [69,70] |

BCL-2 = B-cell CLL/lymphoma 2; DHFR = dihydrofolate reductase; HES1 = hairy/enhancer of split 1; L = leukemic; LOX = lysyl oxidase; NL = normal-like; RB1 = retinoblastoma 1.

NPM1 compared with other leukemic and nonleukemic cells with wt *NPM1* (Fig. 3A). In contrast, *MDM4* expression was lower in mutated OCI/AML3 cells than in other wt cells (Fig. 3B). To prove the effect of *miR-10a* overexpression by functional studies, we chose K562 cells for further studies because these cells express low endogenous levels

of *miR-10a* (see also Fig. 4A). We conducted a microarray experiment to compare whole genome expression of K562 cells transfected with *pre-miR-10a* with that of cells transfected with a negative control miRNA. We identified 130 transcripts with at least 1.5-fold downregulation after *pre-miR-10a* transfection. In contrast, only 30 genes were

Table 3. Characteristics of 89 AML (IR) patients investigated for *miR-10a* expression

| | <i>miR-10a</i> | | | <i>p</i> Value |
|-------------------------------------|----------------|--------------|--------------|----------------|
| | n = 89 | ≤Median | >Median | |
| Age 60 y or younger, n (%) | 65 (73) | 37 (57) | 28 (43) | |
| Sex (female) (%) | 37 (42) | 19 (51) | 18 (49) | |
| WBC, median (range) | 64 (2.8–380) | 48 (2.8–350) | 84 (4.6–380) | |
| BM blast, median (range) | 78 (15–96) | 77 (15–96) | 78.5 (39–95) | |
| FAB, n (%) | | | | |
| M0 | 2 (2) | 2 (100) | 0 (0) | |
| M1 | 29 (33) | 15 (52) | 14 (48) | |
| M2 | 22 (25) | 12 (55) | 10 (45) | |
| M4 | 10 (11) | 4 (40) | 6 (60) | |
| M4eo | 3 (3) | 3 (100) | 0 (0) | |
| M5a | 17 (19) | 7 (41) | 10 (59) | |
| M5b | 4 (5) | 2 (50) | 2 (50) | |
| RAEB-T | 2 (2) | 2 (100) | 0 (0) | |
| de novo, n (%) | 84 (94) | 44 (52) | 40 (48) | |
| MDS, n (%) | 5 (6) | 3 (60) | 2 (40) | |
| CD34%, median (range) | 14 (0–96) | 41 (0–95) | 3.5 (0–96) | <0.0001 |
| CD14%, median (range) | 8 (0–74) | 8 (0–66) | 7 (0–74) | |
| <i>NPM1</i> mutant, n (%) | 36 (40) | 7 (19) | 29 (81) | <0.0001 |
| <i>FLT3</i> -ITD, n (%) | 37 (42) | 19 (51) | 18 (49) | |
| <i>FLT3/D835</i> , n (%) | 11 (12) | 5 (45) | 6 (55) | |
| Extramedullary manifestation, n (%) | 15 (18) | 3 (7) | 12 (27) | 0.01 |

FAB = French-American-British association; MDS = myelodysplastic syndrome; *NPM1* = nucleophosmin 1; RAEB-T = refractory anemia with excess blasts in transformation; WBC = white blood cells.

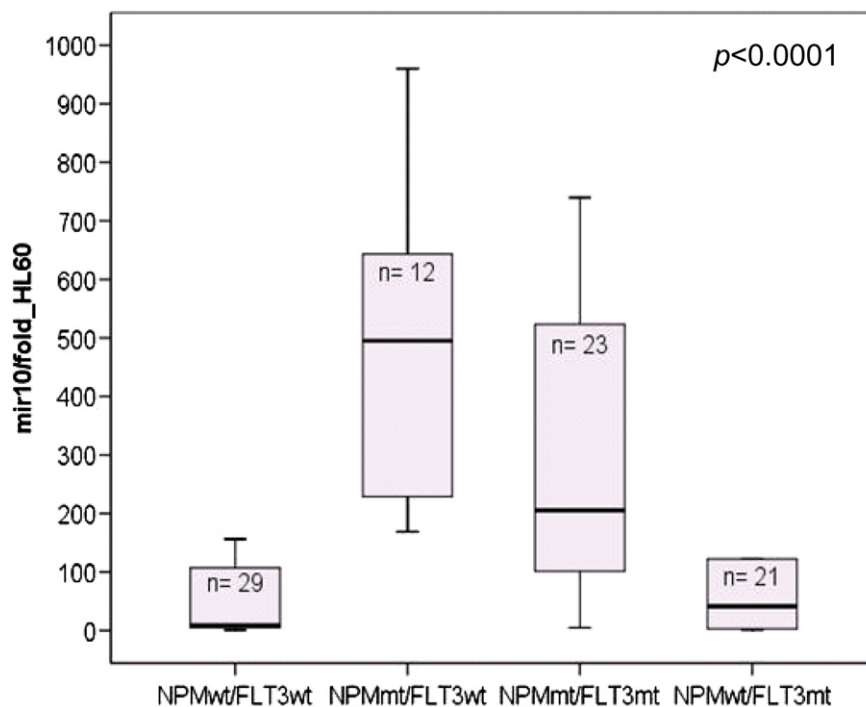


Figure 2. Expression of *mir-10a* in AML patients with IR cytogenetics according to their *NPM1* or *FLT3*-ITD mutational status. Expression levels of *mir-10a* in AML patients ($n = 89$) with IR cytogenetics; expression levels were determined by qRT-PCR using 5S as an internal control; values were calculated according to the $2^{-\Delta\Delta CT}$ method; the HL60 cell line served as an internal control; *NPMwt*, no mutation in exon12 of *NPM1*; *FLT3wt*, no TK or ITD mutation; *NPMmt*, mutated *NPM1*; *FLT3mt*, either TK or ITD mutation in *FLT3* ($p < 0.001$; Kruskal-Wallis H-test for continuous variables).

upregulated to > 1.5 -fold in cells transfected with *pre-miR-10a* (see [Supplementary Table E4](#); online only, available at www.exphem.org).

One of the most strongly influenced genes downregulated by *pre-miR-10a* was *MDM4* (see [Supplementary Table E4](#); online only, available at www.exphem.org). For validation, we next analyzed the expression levels of *MDM4* in HeLa and K562 cells after transient transfection of *pre-miR-10a*. Here, we observed that *MDM4* protein levels were downregulated after *pre-miR-10a* transfection (Fig. 3C). To verify a direct effect of *miR-10a* on *MDM4* regulation, we cloned wt and two mutants of the putative *miR-10a* binding site out of the 3'UTR of *MDM4* into the 3'UTR of a luciferase gene and performed luciferase assays with *pre-* and *anti-miR-10a*-miRNA. Reporter vector containing the wt binding site out of the *MDM4* gene showed a reduction in luciferase activity after cotransfection with *pre-miR-10a*. This was not observed when reporter vectors with a mutated binding site were used, indicating a direct action of *miR-10a* on *MDM4* 3'UTR (Fig. 3D).

To further characterize functional consequences of differential *miR-10a* expression, we transfected OCI/AML3 cells with inhibitory *anti-miR-10a* molecules. *Mir-10a* modulation resulted in altered growth characteristics as compared to the respective control, as inhibition of *miR-10a* resulted in partial resistance to both TRAIL and ATRA treatment ([Supplementary Figure E2](#); online only, available at www.exphem.org).

Finally, we investigated *MDM4* expression levels in AML (IR) patients ($n = 143$) with mutated *NPM1* ($n = 70$) as compared to those with wt *NPM1* gene ($n = 73$). *MDM4* expression levels in patients with a mutated *NPM1* gene showed a tendency for lower expression in comparison to wt *NPM1* (Fig. 4A; $p = 0.07$). Furthermore, Western blot analyses of 16 AML samples (mutated *NPM1*, $n = 8$ and *NPM1* wt, $n = 8$) demonstrated a clear reduction of *MDM4* expression in most *NPM1* mutated samples (Fig. 4B).

Discussion

The detection of altered expression patterns of miRNAs in cancer patient samples may lead to development of important prognostic indicators and could potentially be used to direct treatment strategies on a case-by-case basis. Importantly, it was recently shown that miRNA expression can be used to distinguish AML and normal BM samples [45] from ALL and AML samples [31]. Results of our studies indicate that each leukemia sample can be classified according to particular mutation, which in turn alter expression of specific miRNAs. To exclude miRNA expression differences associated with chromosomal aberrations in AML patients, we investigated miRNA expression patterns in samples from AML patients with (IR) cytogenetics.

We used a microarray-based approach to screen for potential differences in miRNA expression in AML (IR) samples vs. normal BM samples. Heterogeneity of miRNA

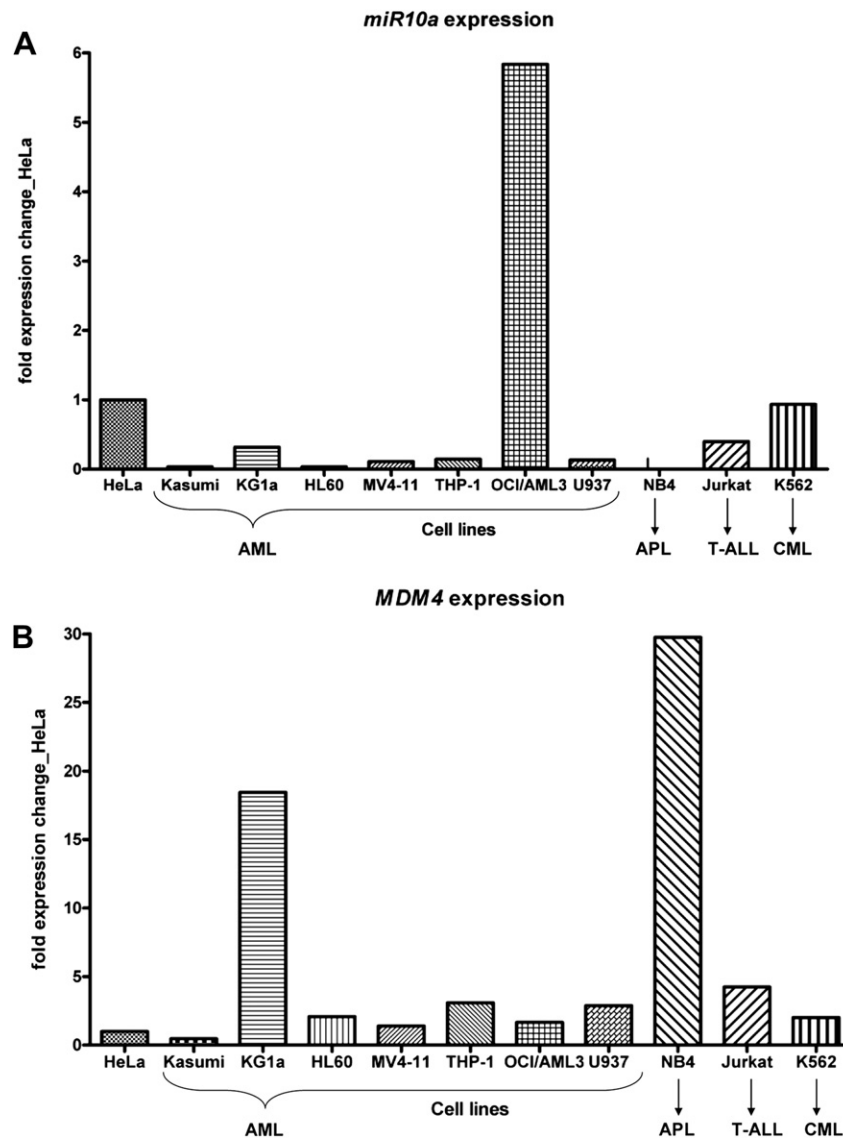


Figure 3. Functional importance of *miR-10a*. (A) Expression of *miR-10a* in different cell-lines was determined by qRT-PCR. Results are shown as relative units compared with the determination in HeLa cells. (B) Expression of *MDM4* in different cell lines was determined by qRT-PCR. Results are shown as relative units compared with the determination in HeLa cells.

expression in AML samples was evident. Although most samples showed aberrant miRNA expression, some AML (NL) samples were not easily distinguished from normal BM samples by microarray analysis. Similar results of hierarchical cluster analyses were reported by Mi et al., who showed that normal BM samples could form subclusters within the clusters of AML samples [31]. The authors concluded that their discriminatory miRNAs were rather deregulated in ALL samples in relative to normal control samples. Interestingly, the NL samples identified were associated with the presence of *NPM1* mutation. Proposed data and models exist favoring the hypothesis that *NPM1* mutations display “founder genetic alterations” defining a distinct AML entity, which in the absence of *FLT3*-ITD mutation is associated with a favorable prognosis [46].

This could indicate that AML samples, which cluster with normal BM samples, indicate “early” AML with only few alterations. Alternatively, this could be an argument for a higher differentiation state of the AML *NPM1* mutated samples.

However, the molecular consequences of mutated *NPM1* in AML are incompletely understood. Gene expression profiles of *NPM1* mutant samples have been compared with AML samples containing wt *NPM1* and a strong clustering effect of *NPM1* mutation was observed [18]. These data indicate that the transcriptional program of *NPM1* mutant samples is clearly different from other AML samples with IR characteristics. Distinctive miRNA signatures have been described in *NPM1* mutant AML samples with normal karyotype [47].

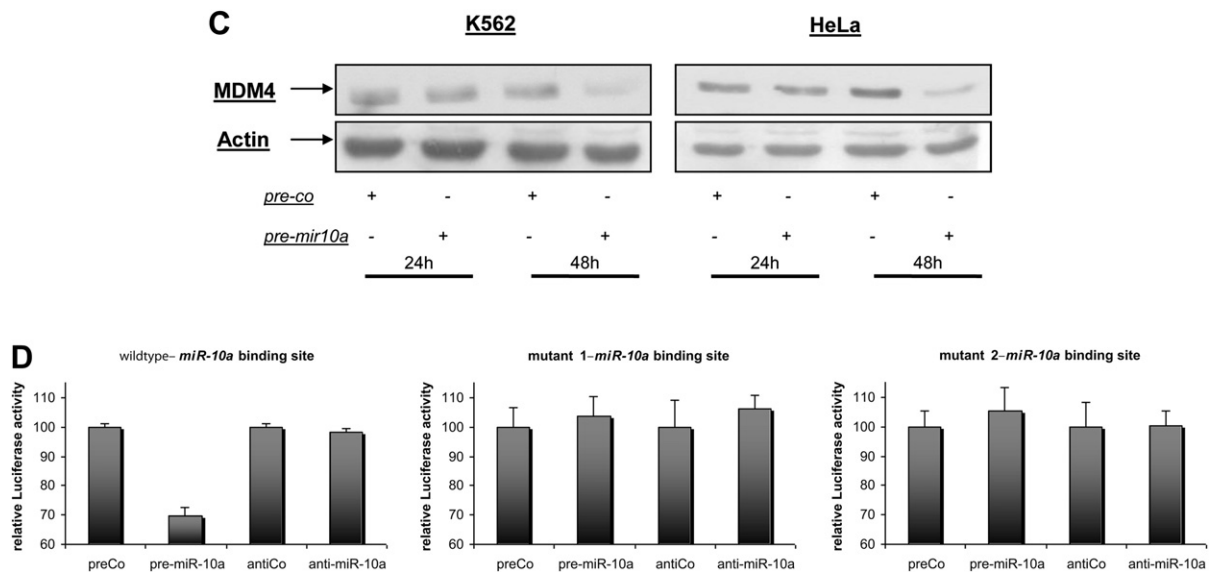


Figure 3. (Continued.) (C) Western Blot of HeLa and K562 cells transfected with either control pre-miRNA or *pre-miR-10a*. Cells were transfected with 50 nmol miRNA constructs using Amaxa technology (T19). After 24 and 48 hours protein was isolated. (D) Luciferase assays in HeLa cells using reporter vectors containing the wt binding site out of the *MDM4* 3'UTR or a mutated variant (mt1, mt2). The cells were cotransfected with the reporter vector and *pre-miR-control-* (*preCo*), *anti-miR-control-* (*antiCo*), *pre-miR-10a-*, and *anti-miR-10a-miRNA*. Firefly luciferase activity was normalized to *Renilla* luciferase activity. Results for luciferase experiments shown, are representative for n = 5 independent experiments.

The results presented confirm previous findings by showing that *miR-10a* is specifically overexpressed in *NPM1* mutant AML samples [47]. Recently, Garzon et al. detected high *miR-10a* expression levels in CD34⁺ hematopoietic progenitor cell samples, which decreased during the in vitro differentiation of megakaryocytes [48]. Moreover, a cluster of miRNAs, including *miR-10a*, was upregulated in AML patients with normal karyotype [34].

Ma et al. found that *miR-10b* is involved in migration of malignant cells, resulting in augmented metastasis rates [49]. *NPM1* mutations are known to correlate with extramedullary involvement (e.g., leukemic manifestations in soft tissue, skin, or organs) in AML [10]. Analyzing our 89 AML (IR) patient samples in which *miR-10a* expression was investigated, we found 15 patients (18%) with extramedullary manifestation of AML at diagnosis, of which 13 patients (87%) harbored mutated *NPM1* (Table 3).

MiR-10a overexpression in *NPM1* mutant AML samples could be a consequence of the transcriptional regulation of a stem cell program. Several groups have described gene expression patterns in *NPM1* mutant AML samples [18,19] and found that *NPM1* mutations are associated with the transcriptional activation of *homeobox* (*HOX*) gene clusters. *MiR-10a* is located within *HOXB* cluster (between *HOXB4* and *HOXB5*) and, as this location is conserved even in invertebrates, it indicates functionality of the genetic region [50]. Mansfield et al. [50] observed coexpression of *HOXB4* and *miR-10a* (located 3-prime to *HOXB4*) in developing mouse embryos, and concluded that *miR-10a* and *HOXB* genes were possibly regulated by common transcriptional mechanisms. Consistent with

previous studies, we observed a strong association between *miR-10a* and *HOXB4* expression in *NPM1* mutant samples (data not shown) [47].

There have only been a limited number of reports that define a specific biological property for *miR-10a*. To identify potential target genes, we conducted microarray studies that detected *MDM4* downregulation. Thus, one explanation for the observed effect, i.e., *miR-10a* overexpression in *NPM1* mutant AML samples can impact cellular defense mechanisms, is *MDM4* downregulation, which is a known mediator of cellular stress that interferes with p53 activation. Because normal *NPM1* function includes stabilization of p53 in the nucleus upon DNA damage [51], it has been suggested that mutated *NPM1* might interfere with these properties [6]. TRAIL induces apoptosis in malignant cells, but not normal cells, while ATRA inhibits cell proliferation and induces differentiation and apoptosis in various ways [52,53]. We could show that partial resistance to both TRAIL and ATRA treatment was induced by *miR-10a* modulation in *NPM1*-mutated OCI/AML3 cells.

MDM4 and MDM2 are critical cellular proteins that balance p53 activation in a nonredundant manner (for review see [54]). MDM4 has been shown to repress p53-mediated transcriptional activation apparently by a direct interaction with p53 at its promoter binding sites [55]. This activity is in contrast to MDM2-mediated p53 degradation and may explain the nonredundant effects of interfering with the two structurally related proteins. There is currently no information on MDM4 expression and activity in AML patients. In contrast, the effect of mutated *NPM1* may depend in part of its inhibitory effect on the

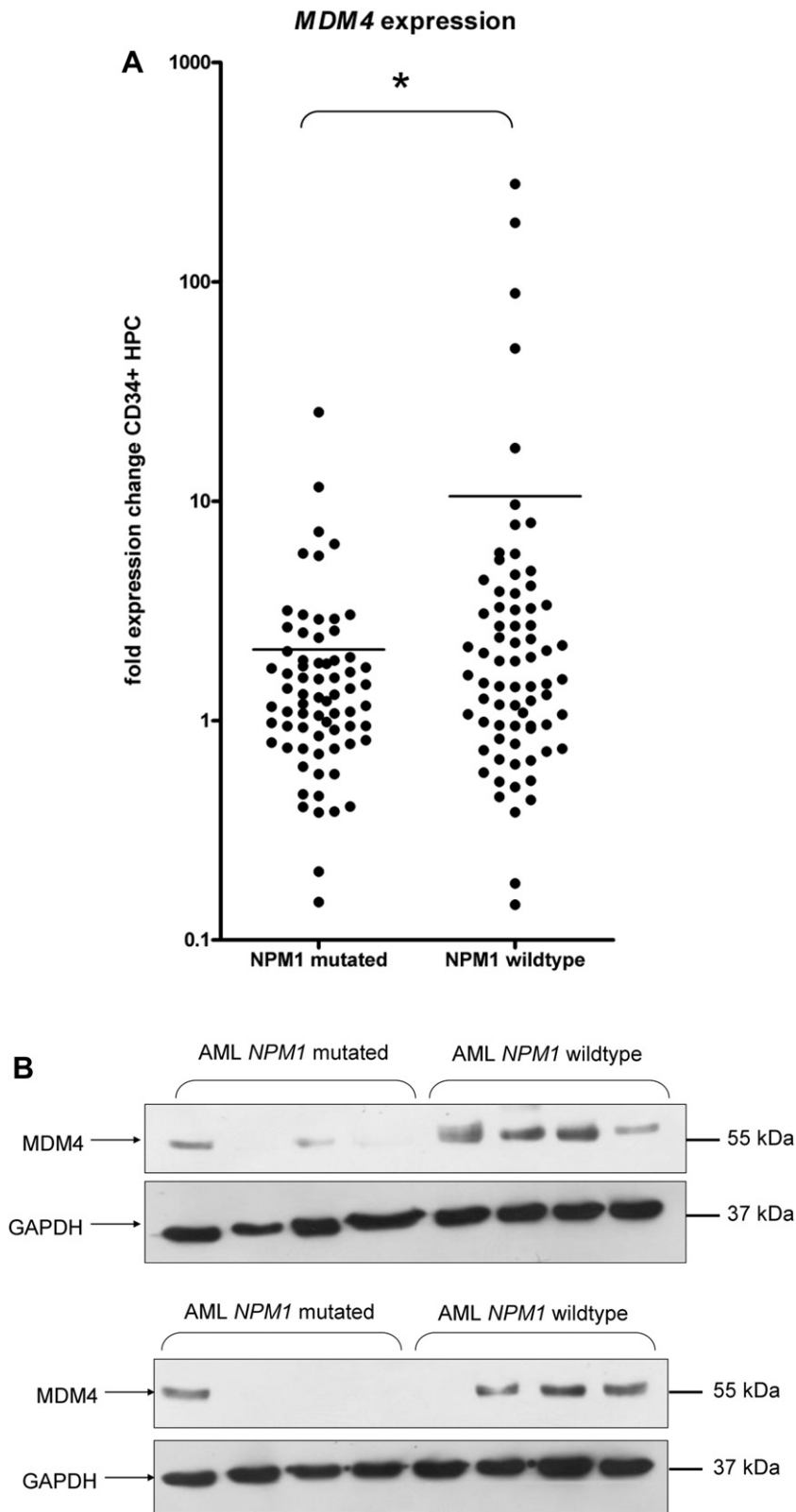


Figure 4. Distribution of *miR-10a* and *MDM4* in AML. (A) Expression of *MDM4* mRNA in AML patients with *NPM1* mutations (*NPM1* mt., $n = 70$) and wt *NPM1* (*NPM1* wt., $n = 73$), determined by qRT-PCR. Results are shown as relative units compared to the expression in CD34⁺ HPCs. $*p = 0.07$; unpaired two-tailed *t*-test. (B) Expression of *MDM4* protein in AML patients with *NPM1* mutations (*NPM1* mt., $n = 8$) and wt *NPM1* (*NPM1* wt., $n = 8$), determined by Western blot analysis.

tumor suppressor ARF, which has been shown to localize in the cytoplasm in association with mutated NPM1. However, additional effects of mutated NPM1 were suspected in this study [56]. Therefore, MDM4 inactivation could be one explanation for the observed complex activity of mutated NPM1. Recently, Harutyunyan et al. demonstrated that chromosome 1q amplifications, harboring the *MDM4* gene, in postmyeloproliferative AML were significantly associated with transformation to AML as compared to chronic-phase myeloproliferative neoplasms [57]. Furthermore, elevated protein levels of the two p53-regulators, MDM2 and MDM4 have been shown to influence the sensitivities of MDM2 inhibitors, such as Nutlins and the MI-series [58]. Because there exist multiple molecular mechanisms that influence the sensitivity and resistance to MDM2 inhibitors, the regulatory mechanisms through miRNAs in this context warrant further investigation [59]. Because our analysis of AML (IR) patients showed a tendency toward lower *MDM4* gene expression data in patients with mutated NPM1 but did not reach statistical significance, we speculate that there may exist other influencing—yet to be discovered—factors that might contribute to these pathophysiological mechanisms.

In conclusion, our results indicate that AML patients with IR characteristics and miRNA array clusters similar to that of normal BM donors, harboring NPM1 mutations have high *miR-10a* expression levels. Finally, we identified *MDM4* to be a target of *miR-10a* in patients with NPM1 mutations, which has been delineated in AML for the first time, to the best of our knowledge. Based on these studies the clinical impact of *miR-10a* and *MDM4* in AML warrants further investigations.

Conflict of interest disclosure

No financial interest/relationships with financial interest relating to the topic of this article have been declared.

Acknowledgments

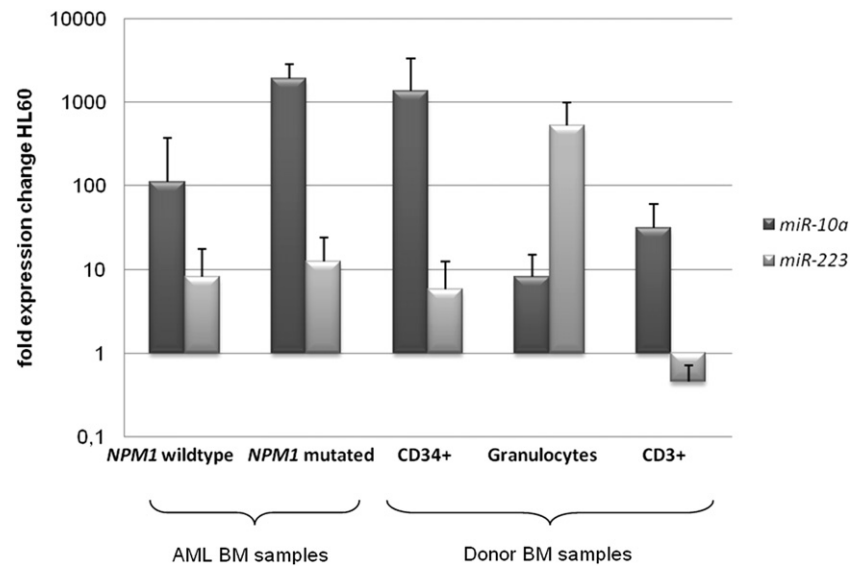
The study was supported in part by a grant from the Centre for Regenerative Therapies Dresden CRTD (T.I.), Deutsche Forschungsgemeinschaft (DFG) Transregio 17 project C3 (A.N.), German Carreras Leukemia Foundation (A.N.), and DFG SFB 655 (F.S., M.B., G.E., and T.I.). The skillful technical assistance of Claudia Dill, Anja Liebkopf, and Maria Schmiedgen is highly acknowledged.

References

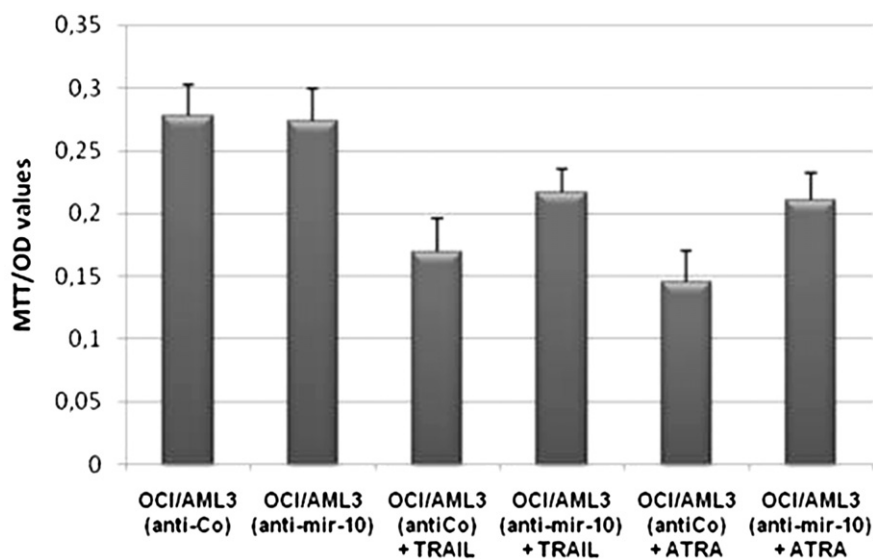
- Lowenberg B. Acute myeloid leukemia: the challenge of capturing disease variety. *Hematology Am Soc Hematol Educ Program*. 2008;1–11.
- Bloomfield CD, Shuma C, Regal L, et al. Long-term survival of patients with acute myeloid leukemia: a third follow-up of the Fourth International Workshop on Chromosomes in Leukemia. *Cancer*. 1997; 80:2191–2198.
- Mrozek K, Marcucci G, Paschka P, Whitman SP, Bloomfield CD. Clinical relevance of mutations and gene-expression changes in adult acute myeloid leukemia with normal cytogenetics: are we ready for a prognostically prioritized molecular classification? *Blood*. 2007; 109:431–448.
- Kiyoi H, Naoe T, Nakano Y, et al. Prognostic implication of FLT3 and N-RAS gene mutations in acute myeloid leukemia. *Blood*. 1999;93: 3074–3080.
- Pabst T, Mueller BU, Zhang P, et al. Dominant-negative mutations of CEBPA, encoding CCAAT/enhancer binding protein- α (CEBP α), in acute myeloid leukemia. *Nat Genet*. 2001;27:263–270.
- Falini B, Mecucci C, Tiacci E, et al. Cytoplasmic nucleophosmin in acute myelogenous leukemia with a normal karyotype. *N Engl J Med*. 2005;352:254–266.
- Frohling S, Schlenk RF, Breitruck J, et al. Prognostic significance of activating FLT3 mutations in younger adults (16 to 60 years) with acute myeloid leukemia and normal cytogenetics: a study of the AML Study Group Ulm. *Blood*. 2002;100:4372–4380.
- Kottaridis PD, Gale RE, Frew ME, et al. The presence of a FLT3 internal tandem duplication in patients with acute myeloid leukemia (AML) adds important prognostic information to cytogenetic risk group and response to the first cycle of chemotherapy: analysis of 854 patients from the United Kingdom Medical Research Council AML 10 and 12 trials. *Blood*. 2001;98:1752–1759.
- Thiede C, Steudel C, Mohr B, et al. Analysis of FLT3-activating mutations in 979 patients with acute myelogenous leukemia: association with FAB subtypes and identification of subgroups with poor prognosis. *Blood*. 2002;99:4326–4335.
- Dohner K, Schlenk RF, Habdank M, et al. Mutant nucleophosmin (NPM1) predicts favorable prognosis in younger adults with acute myeloid leukemia and normal cytogenetics: interaction with other gene mutations. *Blood*. 2005;106:3740–3746.
- Schnittger S, Schoch C, Kern W, et al. Nucleophosmin gene mutations are predictors of favorable prognosis in acute myelogenous leukemia with a normal karyotype. *Blood*. 2005;106:3733–3739.
- Thiede C, Koch S, Creutzig E, et al. Prevalence and prognostic impact of NPM1 mutations in 1485 adult patients with acute myeloid leukemia (AML). *Blood*. 2006;107:4011–4020.
- Brandts CH, Sargin B, Rode M, et al. Constitutive activation of Akt by FLT3 internal tandem duplications is necessary for increased survival, proliferation, and myeloid transformation. *Cancer Res*. 2005;65:9643–9650.
- Levis M, Pham R, Smith BD, Small D. In vitro studies of a FLT3 inhibitor combined with chemotherapy: sequence of administration is important to achieve synergistic cytotoxic effects. *Blood*. 2004; 104:1145–1150.
- Cheng K, Grisendi S, Clohessy JG, et al. The leukemia-associated cytoplasmic nucleophosmin mutant is an oncogene with paradoxical functions: Arf inactivation and induction of cellular senescence. *Oncogene*. 2007;26:7391–7400.
- Colombo E, Bonetti P, Lazzerini Denchi E, et al. Nucleophosmin is required for DNA integrity and p19Arf protein stability. *Mol Cell Biol*. 2005;25:8874–8886.
- Alcalay M, Tiacci E, Bergomas R, et al. Acute myeloid leukemia bearing cytoplasmic nucleophosmin (NPMc+ AML) shows a distinct gene expression profile characterized by up-regulation of genes involved in stem-cell maintenance. *Blood*. 2005;106:899–902.
- Mullighan CG, Kennedy A, Zhou X, et al. Pediatric acute myeloid leukemia with NPM1 mutations is characterized by a gene expression profile with dysregulated HOX gene expression distinct from MLL-rearranged leukemias. *Leukemia*. 2007;21:2000–2009.
- Bullinger L, Dohner K, Bair E, et al. Use of gene-expression profiling to identify prognostic subclasses in adult acute myeloid leukemia. *N Engl J Med*. 2004;350:1605–1616.
- Radmacher MD, Marcucci G, Ruppert AS, et al. Independent confirmation of a prognostic gene-expression signature in adult acute

- myeloid leukemia with a normal karyotype: a Cancer and Leukemia Group B study. *Blood*. 2006;108:1677–1683.
21. Bartel DP. MicroRNAs: genomics, biogenesis, mechanism, and function. *Cell*. 2004;116:281–297.
 22. Lewis BP, Burge CB, Bartel DP. Conserved seed pairing, often flanked by adenosines, indicates that thousands of human genes are microRNA targets. *Cell*. 2005;120:15–20.
 23. Eulalio A, Huntzinger E, Izaurralde E. Getting to the root of miRNA-mediated gene silencing. *Cell*. 2008;132:9–14.
 24. Hornstein E, Mansfield JH, Yekta S, et al. The microRNA miR-196 acts upstream of Hoxb8 and Shh in limb development. *Nature*. 2005;438:671–674.
 25. Hornstein E, Shomron N. Canalization of development by microRNAs. *Nat Genet.*. 2006;38(suppl):S20–S24.
 26. Chen CZ, Li L, Lodish HF, Bartel DP. MicroRNAs modulate hematopoietic lineage differentiation. *Science*. 2004;303:83–86.
 27. Fazi F, Rosa A, Fatica A, et al. A minicircuitry comprised of microRNA-223 and transcription factors NF1-A and C/EBPalpha regulates human granulopoiesis. *Cell*. 2005;123:819–831.
 28. Fukao T, Fukuda Y, Kiga K, et al. An evolutionarily conserved mechanism for microRNA-223 expression revealed by microRNA gene profiling. *Cell*. 2007;129:617–631.
 29. Garzon R, Pichiorri F, Palumbo T, et al. MicroRNA gene expression during retinoic acid-induced differentiation of human acute promyelocytic leukemia. *Oncogene*. 2007;26:4148–4157.
 30. Lu J, Getz G, Miska EA, et al. MicroRNA expression profiles classify human cancers. *Nature*. 2005;435:834–838.
 31. Mi S, Lu J, Sun M, et al. MicroRNA expression signatures accurately discriminate acute lymphoblastic leukemia from acute myeloid leukemia. *Proc Natl Acad Sci U S A*. 2007;104:19971–19976.
 32. Calin GA, Croce CM. Chromosomal rearrangements and microRNAs: a new cancer link with clinical implications. *J Clin Invest*. 2007;117:2059–2066.
 33. Fazi F, Racanicchi S, Zardo G, et al. Epigenetic silencing of the myelopoiesis regulator microRNA-223 by the AML1/ETO oncoprotein. *Cancer Cell*. 2007;12:457–466.
 34. Garzon R, Volinia S, Liu CG, et al. MicroRNA signatures associated with cytogenetics and prognosis in acute myeloid leukemia. *Blood*. 2008;111:3183–3189.
 35. Schaich M, Koch R, Soucek S, Repp R, Ehninger G, Illmer T. A sensitive model for prediction of relapse in adult acute myeloid leukaemia with t(8;21) using white blood cell count, CD56 and MDR1 gene expression at diagnosis. *Br J Haematol*. 2004;125:477–479.
 36. Schaich M, Ritter M, Illmer T, et al. Mutations in ras proto-oncogenes are associated with lower mdrl gene expression in adult acute myeloid leukaemia. *Br J Haematol*. 2001;112:300–307.
 37. Quentmeier H, Martelli MP, Dirks WG, et al. Cell line OCI/AML3 bears exon-12 NPM gene mutation-A and cytoplasmic expression of nucleophosmin. *Leukemia*. 2005;19:1760–1767.
 38. Shingara J, Keiger K, Shelton J, et al. An optimized isolation and labeling platform for accurate microRNA expression profiling. *RNA*. 2005;11:1461–1470.
 39. Livak KJ, Schmittgen TD. Analysis of relative gene expression data using real-time quantitative PCR and the 2(-Delta Delta C(T)) Method. *Methods*. 2001;25:402–408.
 40. Stolzel F, Steudel C, Oelschlagel U, et al. Mechanisms of resistance against PKC412 in resistant FLT3-ITD positive human acute myeloid leukemia cells. *Ann Hematol*; 2010.
 41. Illmer T, Schaich M, Platzbecker U, et al. P-glycoprotein-mediated drug efflux is a resistance mechanism of chronic myelogenous leukemia cells to treatment with imatinib mesylate. *Leukemia*. 2004;18:401–408.
 42. Killian PJ, Sherlock G, Iyer VR. The Longhorn Array Database (LAD): an open-source, MIAME compliant implementation of the Stanford Microarray Database (SMD). *BMC Bioinformatics*. 2003;4:32.
 43. Hochberg Y, Benjamini Y. More powerful procedures for multiple significance testing. *Stat Med*. 1990;9:811–818.
 44. Vaquerizas JM, Conde L, Yankilevich P, et al. GEPAS, an experiment-oriented pipeline for the analysis of microarray gene expression data. *Nucleic Acids Res.*. 2005;33:W616–W620.
 45. Isken F, Steffen B, Merk S, et al. Identification of acute myeloid leukaemia associated microRNA expression patterns. *Br J Haematol*. 2008;140:153–161.
 46. Falini B, Nicoletti I, Martelli MF, Mecucci C. Acute myeloid leukemia carrying cytoplasmic/mutated nucleophosmin (NPMc+ AML): biologic and clinical features. *Blood*. 2007;109:874–885.
 47. Garzon R, Garofalo M, Martelli MP, et al. Distinctive microRNA signature of acute myeloid leukemia bearing cytoplasmic mutated nucleophosmin. *Proc Natl Acad Sci U S A*. 2008;105:3945–3950.
 48. Garzon R, Pichiorri F, Palumbo T, et al. MicroRNA fingerprints during human megakaryocytopoiesis. *Proc Natl Acad Sci U S A*. 2006;103:5078–5083.
 49. Ma L, Teruya-Feldstein J, Weinberg RA. Tumour invasion and metastasis initiated by microRNA-10b in breast cancer. *Nature*. 2007;449:682–688.
 50. Mansfield JH, Harfe BD, Nissen R, et al. MicroRNA-responsive ‘sensor’ transgenes uncover Hox-like and other developmentally regulated patterns of vertebrate microRNA expression. *Nat Genet*. 2004;36:1079–1083.
 51. Colombo E, Marine JC, Danovi D, Falini B, Pelicci PG. Nucleophosmin regulates the stability and transcriptional activity of p53. *Nat Cell Biol*. 2002;4:529–533.
 52. Altucci L, Gronemeyer H. The promise of retinoids to fight against cancer. *Nat Rev Cancer*. 2001;1:181–193.
 53. Wiley SR, Schooley K, Smolak PJ, et al. Identification and characterization of a new member of the TNF family that induces apoptosis. *Immunity*. 1995;3:673–682.
 54. Kruse JP, Gu W. Modes of p53 regulation. *Cell*. 2009;137:609–622.
 55. Marine JC, Francoz S, Maetens M, Wahl G, Toledo F, Lozano G. Keeping p53 in check: essential and synergistic functions of Mdm2 and Mdm4. *Cell Death Differ*. 2006;13:927–934.
 56. den Besten W, Kuo ML, Williams RT, Sherr CJ. Myeloid leukemia-associated nucleophosmin mutants perturb p53-dependent and independent activities of the Arf tumor suppressor protein. *Cell Cycle*. 2005;4:1593–1598.
 57. Harutyunyan A, Klampfl T, Cazzola M, Kralovics R. p53 lesions in leukemic transformation. *N Engl J Med*. 2011;364:488–490.
 58. Francoz S, Froment P, Bogaerts S, et al. Mdm4 and Mdm2 cooperate to inhibit p53 activity in proliferating and quiescent cells in vivo. *Proc Natl Acad Sci U S A*. 2006;103:3232–3237.
 59. Long J, Parkin B, Ouillette P, et al. Multiple distinct molecular mechanisms influence sensitivity and resistance to MDM2 inhibitors in adult acute myelogenous leukemia. *Blood*. 2010;116:71–80.
 60. Mishra PJ, Humeniuk R, Longo-Sorbello GS, Banerjee D, Bertino JR. A miR-24 microRNA binding-site polymorphism in dihydrofolate reductase gene leads to methotrexate resistance. *Proc Natl Acad Sci U S A*. 2007;104:13513–13518.
 61. Wang Q, Huang Z, Xue H, et al. MicroRNA miR-24 inhibits erythropoiesis by targeting activin type I receptor ALK4. *Blood*. 2008;111:588–595.
 62. Felli N, Fontana L, Pelosi E, et al. MicroRNAs 221 and 222 inhibit normal erythropoiesis and erythroleukemic cell growth via kit receptor down-modulation. *Proc Natl Acad Sci U S A*. 2005;102:18081–18086.
 63. le Sage C, Nagel R, Egan DA, et al. Regulation of the p27(Kip1) tumor suppressor by miR-221 and miR-222 promotes cancer cell proliferation. *EMBO J*. 2007;26:3699–3708.
 64. Christoffersen NR, Silahatoglu A, Orom UA, Kauppinen S, Lund AH. miR-200b mediates post-transcriptional repression of ZFX1B. *RNA*. 2007;13:1172–1178.
 65. Liu H, Brannon AR, Reddy AR, et al. Identifying mRNA targets of microRNA dysregulated in cancer: with application to clear cell Renal Cell Carcinoma. *BMC Syst Biol*. 2010;4:51.

66. Cimmino A, Calin GA, Fabbri M, et al. miR-15 and miR-16 induce apoptosis by targeting BCL2. *Proc Natl Acad Sci U S A*. 2005;102:13944–13949.
67. Kulshreshtha R, Ferracin M, Wojcik SE, et al. A microRNA signature of hypoxia. *Mol Cell Biol*. 2007;27:1859–1867.
68. Kimura H, Kawasaki H, Taira K. Mouse microRNA-23b regulates expression of Hes1 gene in P19 cells. *Nucleic Acids Symp Ser (Oxf)*. 2004;213–214.
69. He L, Thomson JM, Hemann MT, et al. A microRNA polycistron as a potential human oncogene. *Nature*. 2005;435:828–833.
70. O'Donnell KA, Wentzel EA, Zeller KI, Dang CV, Mendell JT. c-Myc-regulated microRNAs modulate E2F1 expression. *Nature*. 2005;435:839–843.
71. Jiang Y, Wu Y, Greenlee AR, et al. miR-106a-mediated malignant transformation of cells induced by anti-benzo[a]pyrene-trans-7,8-diol-9,10-epoxide. *Toxicol Sci*. 2011;119:50–60.



Supplementary Figure E1. *Mir-10a* and *miR-223* expression with qRT-PCR AML in AML bone marrow (BM) samples (*NPM1* mutated, n = 7; AML *NPM1* wild-type, n = 8) and healthy BM donors (CD34⁺ [isolated], n = 9; granulocytes, n = 10; and CD3⁺ T cells, n = 10).



Supplementary Figure E2. Influence of external stimuli on OCI/AML3 cells. Cells were transfected with *anti-miR-control* (anti-Co) or *anti-miR-10a*, after 24 hours cells were exposed to either TRAIL or ATRA. After an additional 24 hours, MTT determination was performed.

Supplementary Table E1. Investigated miRNAs as spotted on arrays for AML samples with IR cytogenetics

LET7A
 LET7B
 LET7C
 LET7D
 LET7D-AS
 LET7E
 LET7F-1
 LET7F-2
 LET7G
 LET7I
 MIR1
 MIR100
 MIR101
 MIR103
 MIR105
 MIR106A
 MIR106B
 MIR107
 MIR10A
 MIR122A
 MIR124A
 MIR125A
 MIR125B-1
 MIR126
 MIR126-AS
 MIR127
 MIR128A
 MIR129
 MIR130A
 MIR130B
 MIR132
 MIR133A
 MIR134
 MIR135A
 MIR136
 MIR137
 MIR138
 MIR139
 MIR140
 MIR141
 MIR142-3P
 MIR142-5P
 MIR143
 MIR144
 MIR145
 MIR146
 MIR147
 MIR148A
 MIR149
 MIR150
 MIR151
 MIR152
 MIR153
 MIR154
 MIR155
 MIR15A
 MIR15B
 MIR16
 MIR17-3P
 MIR17-5P
 MIR18
 MIR181A

(continued)

Supplementary Table E1. (continued)

MIR181B
 MIR182
 MIR182-AS
 MIR183
 MIR184
 MIR185
 MIR186
 MIR187
 MIR188
 MIR189
 MIR190
 MIR191
 MIR192
 MIR193
 MIR194
 MIR195
 MIR196-2
 MIR198
 MIR199A
 MIR199A-2
 MIR199A-2-AS
 MIR199A-AS
 MIR19A
 MIR20
 MIR200A
 MIR200B
 MIR201
 MIR202
 MIR203
 MIR204
 MIR205
 MIR206
 MIR207
 MIR208
 MIR21
 MIR210
 MIR211
 MIR212
 MIR213
 MIR214
 MIR215
 MIR216
 MIR217
 MIR218
 MIR219
 MIR22
 MIR221
 MIR222
 MIR223
 MIR224
 MIR23A
 MIR23B
 MIR24
 MIR25
 MIR26A
 MIR27A
 MIR28
 MIR290
 MIR291-3P
 MIR291-5P
 MIR292-3P
 MIR292-5P
 MIR293

(continued)

Supplementary Table E1. (continued)

MIR294
 MIR295
 MIR296
 MIR297-1
 MIR298
 MIR299
 MIR29B
 MIR300
 MIR301
 MIR302
 MIR302B-AS
 MIR302C
 MIR302C-AS
 MIR30A
 MIR30A-AS
 MIR30B
 MIR31
 MIR32
 MIR320
 MIR322
 MIR323
 MIR324-3P
 MIR324-5P
 MIR325
 MIR326
 MIR328
 MIR33
 MIR330
 MIR331
 MIR335
 MIR337
 MIR338
 MIR339
 MIR340
 MIR341
 MIR342
 MIR344
 MIR345
 MIR346
 MIR34A
 MIR34C
 MIR350
 MIR351
 MIR361
 MIR367
 MIR368
 MIR369
 MIR370
 MIR371
 MIR372
 MIR373
 MIR373-AS
 MIR374
 MIR376A
 MIR376B
 MIR380
 MIR381
 MIR382
 MIR383
 MIR384
 MIR409
 MIR410
 MIR411

(continued)

Supplementary Table E1. (continued)

MIR412
 MIR422A
 MIR423
 MIR424
 MIR425
 MIR7
 MIR9
 MIR92
 MIR93
 MIR95
 MIR96
 MIR98
 MIR99A
 MIR99B
 MIR9-AS

Supplementary Table E2. Comparison of qRT-PCR data with semi-quantitative data obtained from microarray datasets

| Correlation | Array data | miR-150 | miR-16 | miR-223 | miR-23a |
|------------------|------------|-----------|----------|----------|-----------|
| miRVana 5S Norm | | 0.091595 | 0.502172 | 0.543302 | 0.547198 |
| PEP mir-24 Norm | | 0.174745 | 0.307471 | 0.21967 | −0.104351 |
| PEP mir-103 Norm | | 0.057825 | 0.395851 | 0.160868 | −0.120495 |
| PEP mir-93 Norm | | −0.042018 | 0.410549 | 0.19493 | −0.033862 |

Data are shown as correlation coefficients.

Supplementary Table E3. Characteristics of AML (IR) patients

| Patient ID | Array group | Age (y) | Sex | FAB subtype | BM blasts (%) | WBC count at diagnosis (Gpt/L) | Karyotype | FLT3-ITD | FLT3-ITD mt/wt ratio | NPM1-mt |
|------------|-------------|---------|-----|-------------|---------------|--------------------------------|---------------------|----------|----------------------|---------|
| 29 | Leukemic | 54 | M | M4 | 92.00 | 224.00 | 46XY | Neg | NA | Pos |
| 30 | Leukemic | 34 | M | M1 | 91.50 | 104.00 | 46XY | Neg | NA | Neg |
| 31 | Leukemic | 22 | F | M1 | 91.50 | 22.60 | 46,XX | Neg | NA | Neg |
| 32 | Leukemic | 28 | M | M1 | 90.50 | 58.60 | 45,X,-Y | Neg | NA | Neg |
| 33 | Leukemic | 36 | M | M1 | 89.50 | 260.00 | 46,XY | Neg | NA | Neg |
| 34 | Leukemic | 33 | M | M5a | 89.50 | 120.00 | 46,XY,del(10)(p1?3) | Neg | NA | Neg |
| 35 | Leukemic | 46 | M | M5a | 88.00 | 41.37 | 46,XY,+Y,+mar | Neg | NA | Neg |
| 37 | Leukemic | 59 | M | M5a | 83.00 | 182.60 | 46,XY | Neg | NA | Pos |
| 39 | Leukemic | 55 | M | M4 | 80.00 | 3.90 | 47,XY | Pos | .04 | Neg |
| 40 | Leukemic | 33 | F | M5a | 88.00 | 131.00 | 46,XX | Pos | 4.6 | Neg |
| 41 | Leukemic | 49 | F | M2 | 90.00 | 153.00 | 46,XX | Pos | .85 | ND |
| 42 | Leukemic | 47 | F | M1 | 93.50 | 72.30 | 46,XX | Pos | 23.4 | Pos |
| 43 | Leukemic | 41 | M | M1 | 86.00 | 78.30 | 46,XY | Pos | .72 | Neg |
| 45 | Leukemic | 52 | M | M1 | 86.00 | 50.00 | 46,XY | Pos | .13 | Pos |
| 46 | Leukemic | 24 | M | M1 | 96.00 | 148.00 | Unknown* | Pos | .81 | Neg |
| 47 | Leukemic | 22 | M | M1 | 90.00 | 29.63 | 47,XY,+4 | Pos | .86 | Neg |
| 27 | Normal-like | 51 | M | M5a | 95.00 | 120.00 | 46,XY | Neg | NA | Pos |
| 28 | Normal-like | 39 | F | M1 | 93.00 | 380.00 | 46,XY | Neg | NA | Pos |
| 36 | Normal-like | 60 | M | M1 | 86.50 | 54.95 | 46,XY | Neg | NA | Pos |
| 38 | Normal-like | 57 | M | M1 | 81.50 | 130.00 | Unknown* | Neg | NA | Pos |
| 44 | Normal-like | 18 | F | M5a | 91.50 | 86.70 | 47,XX,+8 | Pos | 1.67 | Neg |

F = female; FAB = French-American-British association; FLT3 = fms-like tyrosine kinase 3; ITD = internal tandem duplication; mt/wt-ratio = mutant-to-wild-type-ratio; M = male;

NPM1 = nucleophosmin 1; WBC = white blood cells.

*Patients were defined as AML (IR) by performing fluorescence in situ hybridization analysis excluding high-risk cytogenetic features

Supplementary Table E4. Deregulated mRNAs

| Accession ID | Fold change ([pre-mir-10a] vs. [pre-co]) | Regulation ([pre-mir-10a] vs. [pre-co]) | Gene symbol | Gene title |
|--------------|--|---|-----------------|--|
| 211022_s_at | 1,4995008 | Down | <i>ATRX</i> | Alpha thalassemia/mental retardation syndrome X-linked (RAD54 homolog) |
| 221078_s_at | 1,499976 | Down | <i>CCDC88A</i> | Coiled-coil domain containing 88A |
| 200722_s_at | 1,5007571 | Down | <i>CAPRINI</i> | Cell cycle-associated protein 1 |
| 217202_s_at | 1,5011952 | Down | <i>GLUL</i> | Glutamate-ammonia ligase (glutamine synthetase) |
| 213286_at | 1,5034212 | Down | <i>ZFR</i> | Zinc finger RNA binding protein |
| 216855_s_at | 1,5044638 | Down | <i>HNRNPU</i> | Heterogeneous nuclear ribonucleoprotein U (scaffold attachment factor A) |
| 202479_s_at | 1,5052016 | Down | <i>TRIB2</i> | Tribbles homolog 2 (Drosophila) |
| 204770_at | 1,505952 | Down | <i>TAP2</i> | Transporter 2 |
| 220386_s_at | 1,506167 | Down | <i>EML4</i> | Echinoderm microtubule associated protein like 4 |
| 219858_s_at | 1,5078781 | Down | <i>FLJ20160</i> | FLJ20160 protein |
| 222283_at | 1,5086538 | Down | <i>ZNF480</i> | Zinc finger protein 480 |
| 210585_s_at | 1,5097202 | Down | <i>TNPO2</i> | Transportin 2 (importin 3) |
| 220800_s_at | 1,5097871 | Down | <i>TMOD3</i> | Tropomodulin 3 (ubiquitous) |
| 216549_s_at | 1,5099028 | Down | <i>TBC1D22B</i> | TBC1 domain family |
| 208721_s_at | 1,5122412 | Down | <i>ANAPC5</i> | Anaphase promoting complex subunit 5 |
| 214390_s_at | 1,5151955 | Down | <i>BCAT1</i> | Branched chain aminotransferase 1 |
| 211273_s_at | 1,516987 | Down | <i>TBX1</i> | T-box 1 |
| 212008_at | 1,5182364 | Down | <i>UBXD2</i> | UBX domain-containing 2 |
| 211074_at | 1,5187875 | Down | <i>FOLR1</i> | Folate receptor 1 (adult) |
| 214971_s_at | 1,5205553 | Down | <i>ST6GAL1</i> | ST6 beta-galactosamide alpha-2,6-sialyltransferase 1 |
| 201835_s_at | 1,5208024 | Down | <i>PRKAB1</i> | Protein kinase |
| 219558_at | 1,5210507 | Down | <i>ATP13A3</i> | ATPase type 13A3 |
| 213756_s_at | 1,5210936 | Down | <i>HSF1</i> | Heat shock transcription factor 1 |
| 213472_at | 1,5231981 | Down | <i>HNRNPH1</i> | Heterogeneous nuclear ribonucleoprotein H1 (H) |
| 208650_s_at | 1,5232625 | Down | <i>CD24</i> | CD24 molecule |
| 214849_at | 1,5236279 | Down | <i>KCTD20</i> | Potassium channel tetramerization domain containing 20 |
| 205966_at | 1,524531 | Down | <i>TAF13</i> | TAF13 RNA polymerase II |
| 211094_s_at | 1,5279856 | Down | <i>NF1</i> | Neurofibromin 1 |
| 214245_at | 1,5282876 | Down | <i>RPS14</i> | Ribosomal protein S14 |
| 216521_s_at | 1,5292673 | Down | <i>BRCC3</i> | BRCA1/BRCA2-containing complex |
| 215509_s_at | 1,5362564 | Down | <i>BUB1</i> | BUB1 budding uninhibited by benzimidazoles 1 homolog (yeast) |
| 201902_s_at | 1,5372647 | Down | <i>YY1</i> | YY1 transcription factor |
| 214190_x_at | 1,5377111 | Down | <i>GGA2</i> | Golgi associated |
| 211220_s_at | 1,538794 | Down | <i>HSF2</i> | Heat shock transcription factor 2 |
| 207686_s_at | 1,5416571 | Down | <i>CASP8</i> | Caspase 8 |
| 215099_s_at | 1,5421553 | Down | <i>RXRβ</i> | Retinoid X receptor |
| 210932_s_at | 1,5472378 | Down | <i>RNF6</i> | Ring finger protein (C3H2C3 type) 6 |
| 201971_s_at | 1,5487323 | Down | <i>ATP6V1A</i> | ATPase |
| 201151_s_at | 1,5501565 | Down | <i>MBNL1</i> | Muscleblind-like (Drosophila) |
| 201337_s_at | 1,550751 | Down | <i>VAMP3</i> | Vesicle-associated membrane protein 3 (cellubrevin) |
| 205835_s_at | 1,5521927 | Down | <i>YTHDC2</i> | YTH domain containing 2 |
| 211574_s_at | 1,5548548 | Down | <i>CD46</i> | CD46 molecule |
| 214697_s_at | 1,5671521 | Down | <i>ROD1</i> | ROD1 regulator of differentiation 1 (Schizosaccharomyces <i>Pombe</i>) |
| 205371_s_at | 1,5726333 | Down | <i>DBT</i> | Dihydrolipoamide branched chain transacylase E2 |
| 211090_s_at | 1,5748426 | Down | <i>PRPF4B</i> | PRP4 pre-mRNA processing factor 4 homolog B (yeast) |
| 200841_s_at | 1,5784054 | Down | <i>EPRS</i> | Glutamyl-prolyl-TMA synthetase |
| 201299_s_at | 1,5804567 | Down | <i>MOBK1B</i> | Mob1 |
| 215739_s_at | 1,5825475 | Down | <i>TUBGCP3</i> | Tubulin |
| 209456_s_at | 1,5866083 | Down | <i>FBXW11</i> | F-box and WD repeat domain containing 11 |
| 221268_s_at | 1,5916929 | Down | <i>SGPP1</i> | Sphingosine-1-phosphate phosphatase 1 |
| 211088_s_at | 1,5917389 | Down | <i>PLK4</i> | Polo-like kinase 4 (Drosophila) |
| 205018_s_at | 1,5934554 | Down | <i>MBNL2</i> | Muscleblind-like 2 (Drosophila) |
| 210077_s_at | 1,5964437 | Down | <i>SFRS5</i> | Splicing factor |
| 210457_x_at | 1,597052 | Down | <i>HMGA1</i> | High mobility group AT-hook 1 |
| 214216_s_at | 1,5996033 | Down | <i>LARP5</i> | La ribonucleoprotein domain family |
| 221638_s_at | 1,6044447 | Down | <i>STX16</i> | Syntaxin 16 |
| 207793_s_at | 1,6099403 | Down | <i>EPB41</i> | Erythrocyte membrane protein band 4.1 (elliptocytosis 1, RH-linked) |
| 200952_s_at | 1,6109558 | Down | <i>CCND2</i> | Cyclin D2 |
| 219872_at | 1,612254 | Down | <i>C4orf18</i> | Chromosome 4 open reading frame 18 |

(continued)

Supplementary Table E4. (continued)

| Accession ID | Fold change ([pre-mir-10a] vs. [pre-co]) | Regulation ([pre-mir-10a] vs. [pre-co]) | Gene symbol | Gene title |
|--------------|--|---|-------------------------------------|--|
| 217445_s_at | 1,6147336 | Down | <i>GART</i> | Phosphoribosylglycinamide formyltransferase |
| 207824_s_at | 1,6155097 | Down | <i>MAZ</i> | MYC-associated zinc finger protein (purine-binding transcription factor) |
| 212574_x_at | 1,6177799 | Down | <i>C19orf6</i> | Chromosome 19 open reading frame 6 |
| 34478_at | 1,6191995 | Down | <i>RAB11B</i> | Rab11b |
| 210317_s_at | 1,6203048 | Down | <i>YWHAE</i> | Tyrosine 3-monooxygenase/tryptophan 5-monooxygenase activation protein |
| 216205_s_at | 1,6223296 | Down | <i>MFN2</i> | Mitofusin 2 |
| 203032_s_at | 1,629594 | Down | <i>FH</i> | Fumarate hydratase |
| 206788_s_at | 1,6300653 | Down | <i>CBFB</i> | Core-binding factor |
| 221628_s_at | 1,6326449 | Down | <i>N-PAC</i> | Cytokine-like nuclear factor n-pac |
| 206241_at | 1,6330737 | Down | <i>KPNA5</i> | Karyopherin alpha 5 (importin alpha 6) |
| 211205_x_at | 1,6347475 | Down | <i>PIP5K1A</i> | Phosphatidylinositol-4-phosphate 5-kinase |
| 210866_s_at | 1,6352849 | Down | <i>CNOT4</i> | CCR4-NOT transcription complex |
| 201559_s_at | 1,6427157 | Down | <i>CLIC4</i> | Chloride intracellular channel 4 |
| 204666_s_at | 1,6431797 | Down | <i>RP5-1000E10.4</i> | Suppressor of IKK epsilon |
| 215236_s_at | 1,6513644 | Down | <i>PICALM</i> | Phosphatidylinositol binding clathrin assembly protein |
| 208097_s_at | 1,6527044 | Down | <i>TXNDC1</i> | Thioredoxin domain containing 1 |
| 212619_at | 1,6556174 | Down | <i>TMEM194</i> | Transmembrane protein 194 |
| 216901_s_at | 1,6561874 | Down | <i>IKZF1</i> | IKAROS family zinc finger 1 (IkaroS) |
| 201211_s_at | 1,6571327 | Down | <i>DDX3X</i> | DEAD (Asp-Glu-Ala-Asp) box polypeptide 3 |
| 209006_s_at | 1,6659354 | Down | <i>C1orf63</i> | Chromosome 1 open reading frame 63 |
| 216985_s_at | 1,668429 | Down | <i>STX3</i> | Syntaxin 3 |
| 204427_s_at | 1,6690917 | Down | <i>TMED2</i> | Transmembrane emp24 domain trafficking protein 2 |
| 214007_s_at | 1,6702452 | Down | <i>TWF1</i> | Twinfilin |
| 220797_at | 1,6732249 | Down | <i>METT10D</i> | Methyltransferase 10 domain containing |
| 215220_s_at | 1,6778793 | Down | <i>TPR</i> | Translocated promoter region (to activated MET oncogene) |
| 218748_s_at | 1,6789892 | Down | <i>EXOC5</i> | Exocyst complex component 5 |
| 202199_s_at | 1,687683 | Down | <i>SRPK1</i> | SFRS protein kinase 1 |
| 210828_s_at | 1,6894844 | Down | ARNT | Aryl hydrocarbon receptor nuclear translocator |
| 200917_s_at | 1,6923304 | Down | <i>SRPR</i> | Signal recognition particle receptor ('docking protein') |
| 206665_s_at | 1,706015 | Down | <i>BCL2L1</i> | BCL2-like 1 |
| 212105_s_at | 1,7068222 | Down | <i>DHX9</i> | DEAH (Asp-Glu-Ala-His) box polypeptide 9 |
| 216915_s_at | 1,7102363 | Down | <i>PTPN12</i> | Protein tyrosine phosphatase |
| 211547_s_at | 1,7120155 | Down | <i>PAFAH1B1</i> | Platelet-activating factor acetylhydrolase |
| 212392_s_at | 1,7138575 | Down | <i>LOC652526///PDE4DIP</i> | Phosphodiesterase 4D interacting protein (myomegalin)///similar to phosphodiesterase 4D interacting protein isoform 2 |
| 214130_s_at | 1,7150333 | Down | <i>PDE4DIP</i> | Phosphodiesterase 4D interacting protein (myomegalin) |
| 211162_x_at | 1,7171289 | Down | <i>SCD</i> | Stearoyl-coa desaturase (delta-9-desaturase) |
| 211016_x_at | 1,7218277 | Down | <i>HSPA4</i> | Heat shock 70-kda protein 4 |
| 217859_s_at | 1,7238463 | Down | <i>SLC39A9</i> | Solute carrier family 39 (zinc transporter) |
| 217870_s_at | 1,7274396 | Down | <i>CMPK1</i> | Cytidine monophosphate (UMP-CMP) kinase 1 |
| 205867_at | 1,7283465 | Down | <i>PTPN11</i> | Protein tyrosine phosphatase, nonreceptor type 11 |
| 206184_at | 1,7298421 | Down | <i>CRKL</i> | V-crk sarcoma virus CT10 oncogene homolog (avian)-like |
| 213548_s_at | 1,7347237 | Down | <i>CDV3</i> | CDV3 homolog (mouse) |
| 214071_at | 1,7373677 | Down | <i>MPPE1</i> | Metallophosphoesterase 1 |
| 208116_s_at | 1,7457724 | Down | <i>MAN1A1</i> | Mannosidase |
| 204560_at | 1,7470237 | Down | <i>FKBP5</i> | FK506 binding protein 5 |
| 216493_s_at | 1,7531601 | Down | <i>IGF2BP3///LOC645468</i> | Insulin-like growth factor 2 mRNA binding protein 3///similar to putative RNA binding protein KOC |
| 215581_s_at | 1,754282 | Down | <i>MCM3AP</i> | Minichromosome maintenance complex component 3-associated protein |
| 208047_s_at | 1,7557199 | Down | <i>NAB1</i> | NGFI-A binding protein 1 (EGR1 binding protein 1) |
| 200796_s_at | 1,7608273 | Down | <i>MCL1</i> | Myeloid cell leukemia sequence 1 (BCL-2-related) |
| 210440_s_at | 1,7636423 | Down | <i>CDC14A</i> | CDC14 cell division cycle 14 homolog A (<i>Saccharomyces Cerevisiae</i>) |
| 203626_s_at | 1,7687414 | Down | <i>SKP2</i> | S-phase kinase-associated protein 2 (p45) |
| 210892_s_at | 1,7765058 | Down | <i>GTF2I</i> | General transcription factor II |
| 209629_s_at | 1,7871082 | Down | <i>NXT2</i> | Nuclear transport factor 2-like export factor 2 |
| 209754_s_at | 1,7933791 | Down | <i>TMPO</i> | Thymopoietin |
| 216902_s_at | 1,8083738 | Down | <i>LOC653390///LOC730092///RRN3</i> | RRN3 RNA polymerase I transcription factor homolog (<i>Saccharomyces Cerevisiae</i>)///RRN3 RNA polymerase I transcription factor homolog (<i>Saccharomyces Cerevisiae</i>) pseudogene |

(continued)

Supplementary Table E4. (continued)

| Accession ID | Fold change ([pre-mir-10a] vs. [pre-co]) | Regulation ([pre-mir-10a] vs. [pre-co]) | Gene symbol | Gene title |
|--------------|--|---|--------------------|--|
| 217176_s_at | 1,809362 | Down | ZFX | Zinc finger protein |
| 205732_s_at | 1,8224169 | Down | NCOA2 | Nuclear receptor coactivator 2 |
| 215150_at | 1,8244326 | Down | <i>YOD1</i> | YOD1 OTU deubiquinating enzyme 1 homolog (<i>S. Cerevisiae</i>) |
| 212142_at | 1,8362669 | Down | MCM4 | Minichromosome maintenance complex component 4 |
| 214786_at | 1,8539861 | Down | MAP3K1 | Mitogen-activated protein kinase kinase kinase 1 |
| 219608_s_at | 1,854201 | Down | FBXO38 | F-box protein 38 |
| 217097_s_at | 1,8662989 | Down | PHTF2 | Putative homeodomain transcription factor 2 |
| 203294_s_at | 1,8703344 | Down | LMAN1 | Lectin |
| 214336_s_at | 1,885618 | Down | COPA | Coatomer protein complex |
| 214975_s_at | 1,9469228 | Down | MTMR1 | Myotubularin related protein 1 |
| 212797_at | 1,983121 | Down | <i>SORT1</i> | Sortilin 1 |
| 221618_s_at | 2,0026515 | Down | LOC728198//TAF9B | TAF9B RNA polymerase II |
| 206943_at | 2,0033834 | Down | <i>TGFBR1</i> | Transforming growth factor |
| 205655_at | 2,0270846 | Down | <i>MDM4</i> | Mdm4 p53 binding protein homolog (mouse) |
| 213606_s_at | 2,1147816 | Down | ARHGDI4 | Rho GDP dissociation inhibitor (GDI) alpha |
| 206579_at | 2,1255388 | Down | ZNF192 | Zinc finger protein 192 |
| 219927_at | 2,2972803 | Down | <i>FCF1</i> | FCF1 small subunit (SSU) processome component homolog (<i>S. Cerevisiae</i>) |
| 212185_x_at | 1,5050669 | Up | MT2A | Metallothionein 2A |
| 212599_at | 1,5079852 | Up | AUTS2 | Autism susceptibility candidate 2 |
| 221478_at | 1,5125571 | Up | BNIP3L | BCL2/adenovirus E1B 19kda interacting protein 3-like |
| 202458_at | 1,5177377 | Up | PRSS23 | Protease |
| 209795_at | 1,5322977 | Up | CD69 | CD69 molecule |
| 206494_s_at | 1,5378845 | Up | ITGA2B | Integrin |
| 214978_s_at | 1,5383469 | Up | PPFIA4 | Protein tyrosine phosphatase |
| 205927_s_at | 1,5472317 | Up | CTSE | Cathepsin E |
| 222024_s_at | 1,5497096 | Up | <i>AKAP13</i> | A kinase (PRKA) anchor protein 13 |
| 213506_at | 1,550675 | Up | F2RL1 | Coagulation factor II (thrombin) receptor-like 1 |
| 220560_at | 1,5588487 | Up | C11orf21 | Chromosome 11 open reading frame 21 |
| 213975_s_at | 1,5607862 | Up | <i>LYZ</i> | Lysozyme (renal amyloidosis) |
| 212614_at | 1,5785391 | Up | ARID5B | AT rich interactive domain 5B (MRF1-like) |
| 207463_x_at | 1,5802315 | Up | PRSS3 | Protease |
| 203695_s_at | 1,5820975 | Up | DFNA5 | Deafness |
| 200872_at | 1,5952313 | Up | S100A10 | S100 calcium binding protein A10 |
| 219403_s_at | 1,629079 | Up | HPSE | Heparanase |
| 208792_s_at | 1,6501576 | Up | CLU | Clusterin |
| 213438_at | 1,6593443 | Up | NFASC | Neurofascin homolog (chicken) |
| 215235_at | 1,6661867 | Up | SPTAN1 | Spectrin |
| 219059_s_at | 1,675863 | Up | <i>LYVE1</i> | Lymphatic vessel endothelial hyaluronan receptor 1 |
| 205626_s_at | 1,6777687 | Up | CALB1 | Calbindin 1 |
| 221211_s_at | 1,7345427 | Up | <i>C21orf7</i> | Chromosome 21 open reading frame 7 |
| 200762_at | 1,7381908 | Up | DPYSL2 | Dihydropyrimidinase-like 2 |
| 219476_at | 1,7981561 | Up | <i>C1orf116</i> | Chromosome 1 open reading frame 116 |
| 215395_x_at | 1,808629 | Up | LOC100134294//TRY6 | Trypsinogen C//hypothetical protein LOC100134294 |
| 219410_at | 1,8366171 | Up | TMEM45A | Transmembrane protein 45A |
| 205402_x_at | 1,8558791 | Up | PRSS2 | Protease |
| 208966_x_at | 1,859521 | Up | IFI16 | Interferon |
| 212063_at | 1,9257536 | Up | CD44 | CD44 molecule (Indian blood group) |
| 202237_at | 2,2827954 | Up | NNMT | Nicotinamide N-methyltransferase |

Deregulated mRNAs containing conserved *miR-10a* binding sites are depicted in bold. Deregulated mRNAs containing poorly conserved *miR-10a* binding sites are depicted in italics.